

## Phase instability, spin fluctuations, and superconductivity in the C15 compound $V_2Zr$

H. Keiber, C. Geibel, B. Renker, H. Rietschel, H. Schmidt, and H. Wühl  
*Kernforschungszentrum Karlsruhe und Universität Karlsruhe, Postfach 3640,  
 D-7500 Karlsruhe, Federal Republic of Germany*

G. R. Stewart

*Los Alamos National Laboratory, Los Alamos, New Mexico 87545*

(Received 3 May 1984)

From low-temperature measurements of the specific heat and the magnetic susceptibility, we determined  $T_c$ ,  $\gamma$ , and  $\chi^{\text{spin}}$  for both the cubic and the rhombohedral phase of the C15 compound  $V_2Zr$ . In addition, neutron-diffraction experiments were performed for a proper identification of these two phases. We found that the martensitic transformation ( $T_M \sim 110$  K) from the cubic to the rhombohedral phase leads to a substantial reduction in  $\gamma$  and  $\chi^{\text{spin}}$ :  $\gamma_{\text{cub}} (\gamma_{\text{rh}}) \sim 23$  (16) mJ/g-at. K<sup>2</sup> and  $\chi_{\text{cub}}^{\text{spin}} (\chi_{\text{rh}}^{\text{spin}}) \sim 2.1 \times 10^{-7}$  ( $1.4 \times 10^{-4}$ ) emu/g-at. In contrast,  $T_c$  is only slightly changed:  $T_c^{\text{cub}} \sim 8.7$  K and  $T_c^{\text{rh}} \sim 8.0$  K. Together with the fact that the "Wilson ratio"  $N(\chi)/N(\gamma) \sim 0.7$  in both phases, we take our findings as clear evidence that in  $V_2Zr$   $T_c$  is limited by spin fluctuations.

### I. INTRODUCTION

A high electronic density of states (DOS) at the Fermi level,  $N(0)$ , favors the onset of superconductivity in two respects. First, since the formation of Cooper pairs is restricted to the immediate neighborhood of the Fermi surface,  $N(0)$  is a direct measure for the number of electrons sharing the superconducting quantum state. In BCS theory, this is reflected by the explicit appearance of  $N(0)$  in the coupling strength,  $\lambda_{\text{BCS}} = N(0)V$ . Second, the interaction  $V$  which is mediated by virtual phonon exchange, is itself a function of  $N(0)$ . A higher  $N(0)$  leads to phonon softening and thus to a higher  $V$ , although this effect may partly be compensated by enhanced screening of the electron-phonon vertex.<sup>1</sup> On the other hand, this phonon softening can culminate in an electronically driven (Jahn-Teller-type) phase transition into a stabler phase with lower  $N(0)$  and thus weaker electron-phonon coupling. Also, changes in  $N(0)$  affect the Coulomb repulsion between the electrons, i.e.,  $\mu^*$ . In particular, in cooperation with Coulomb exchange and correlation, an increasing  $N(0)$  always implies a growing tendency towards itinerant magnetism, thus leading either to a depression of  $T_c$  by spin fluctuations or even to the total quenching of superconductivity.

Combining all these effects, one may imagine situations where for a superconductor,  $T_c$  can still be raised by raising  $N(0)$ , i.e., where  $dT_c/dN(0) > 0$ , as well as situations where  $dT_c/dN(0) < 0$ . In this latter case, the optimum value for  $N(0)$  has already been surpassed, and an increase in  $T_c$  requires a reduction of  $N(0)$ . (Pd may be an example of this rare happening<sup>2</sup>.) Thus, when looking for high- $T_c$  superconductivity within a given class of materials, it is of particular interest to find the point where  $dT_c/dN(0) \sim 0$ , i.e., to meet the optimum conditions for high  $T_c$  with respect to  $N(0)$ .

In this paper, we present experimental evidence for the fact that in the C15 compound  $V_2Zr$ , such an optimum

situation has nearly been achieved. In several respects,  $V_2Zr$  is reminiscent of the high- $T_c$  A15 compounds  $V_3Si$  and  $Nb_3Sn$ . It has a high magnetic susceptibility  $\chi(T)$  with an anomalously large temperature dependence, and it undergoes a martensitic phase transformation from the cubic into a rhombohedral phase below  $T_M \sim 110$  K,<sup>3</sup> while  $V_3Si$  and  $Nb_3Sn$  undergo martensitic transitions to the tetragonal phase at  $\sim 21$  and  $\sim 45$  K, respectively. Actually, recent band-structure calculations<sup>4,5</sup> have shown that the electronic DOS in  $V_2Zr$  is very similar to that in  $V_3Si$ : At  $\epsilon_F$ , its height is about 110 states/spin Ry unit-cell and it has a sharp peak close to  $\epsilon_F$ .

In our experiments, we exploited the fact that the martensitic transformation in  $V_2Zr$  into the rhombohedral phase can be hindered by very small amounts of residual strain or concentration gradients. All our samples underwent the martensitic transformation only partly, thus allowing the simultaneous observation of both phases at low temperatures. By performing neutron scattering experiments and measurements of the magnetic susceptibility and low-temperature specific heat, we were able to assign distinct values for  $T_c$ ,  $\gamma$ , and  $\chi$  to both the cubic and the rhombohedral phase. While there is already experimental information on  $T_c$ ,  $\gamma$ , and  $\chi$  for the rhombohedral phase of  $V_2Zr$ ,<sup>4,6,7</sup> to our knowledge we are the first to present values of  $\gamma$  and  $T_c$  for the cubic phase. Our central result is the finding that the phase transformation into the rhombohedral phase leads to a substantial decrease in  $\gamma$  and  $\chi^{\text{spin}}$ , and hence in  $N(0)$ , while  $T_c$  is lowered by only 0.7 K, thus proving that  $dT_c/dN(0)$  is close to 0 in this compound.

The remainder of the paper is organized into five sections. Sample preparation and characterization are discussed in Sec. II, the neutron scattering experiments in Sec. III. Sections IV and V, respectively, deal with the measurement and evaluation of the specific heat and magnetic susceptibility. In Sec. VI we discuss our results and present our final conclusions.

## II. SAMPLE PREPARATION AND CHARACTERIZATION

The samples were prepared from V and Zr rods with a purity of 99.7% and 99.9%, respectively, purchased from MRC Corporation. The components were weighed to give the  $V_2Zr$  composition and melted in a levitation crucible under vacuum better than  $10^{-5}$  mbar to produce ingots of 5 g. Each ingot was remelted four times to ensure homogeneity. Weight losses were negligible. These as-cast samples showed a microstructure typical of a peritectic decomposition: homogeneously distributed V grains surrounded by a  $V_2Zr$  layer and a  $V_2Zr/\alpha$ -Zr eutectic. The bulk percentage of  $V_2Zr$  phase was less than 30%. After a 120-h heat treatment under argon at 1200°C, metallographic and x-ray analysis revealed mostly single phase  $V_2Zr$  ( $a_0=7.448$  Å) with small amounts of a second phase (~3%). This second phase could be identified as  $V_3Zr_3O_x$  with  $\eta$ -carbide structure as described by Rotella *et al.*<sup>8</sup>

For our investigations, we used four different samples S1 to S4, each of them with an approximate weight of 150 mg. S1, S2, and S4 were taken from different sites of the same ingot, S3 from a different ingot. Though from the same ingot, S1, S2, and S4 differed appreciably in the bulk percentage of material undergoing the martensitic phase transformation into the rhombohedral phase. This is an indication of the strong sensitivity of this structural transition to small concentration gradients or residual strains.

## III. NEUTRON DIFFRACTION

Neutron powder diffraction experiments were performed using a three-axis spectrometer at the ORPHEE reactor in Saclay. The energy of the neutrons was 14.7 meV. Diffraction patterns were taken on S2 and S3 for both the (111) and the (220) reflex in the temperature range  $15 \leq T \leq 300$  K. In the low-temperature rhombohedral phase, the (111) reflex splits into (10.1) and (0.03) (in hexagonal indices) with ratio 3:1, and the (220) reflex into (11.0) and (10.4) with ratio 1:1. We observed both splittings. Figure 1 presents our scattering results on S3 at  $T \sim 15$  K together with a least-squares fit using three Gaussians. Besides the split lines, an unsplit cubic remainder is clearly recognizable. From the ratio  $I_S/I_T$  (where  $I_S$  is intensity in the split lines and  $I_T$  is the total intensity) we determined the fraction of rhombohedral phase,  $p_{rh}$ , to be  $0.88 \pm 0.02$  in S3. From a similar analysis of the scattering results on S2, we obtained  $p_{rh} = 0.7 \pm 0.1$  (see Table I). The large error bar is due to the fact that this sample showed large texture, i.e., the extracted  $p_{rh}$  depended considerably on the sample orientation.

From our scattering results on S3, we also determined the  $c/a$  ratio in the rhombohedral phase. The hexagonal lattice parameters  $a$  and  $c$  are defined by  $a = a_0(1 + \epsilon)/\sqrt{2}$  and  $c = a_0(1 - 2\epsilon)\sqrt{3}$ , where  $a_0$  is the cubic lattice constant and  $\epsilon$  the strain parameter. We found  $c/a = 2.329 \pm 0.001$  ( $\epsilon = 0.017$ ), in very good agreement with the results by Moncton.<sup>9</sup> We note that the asym-

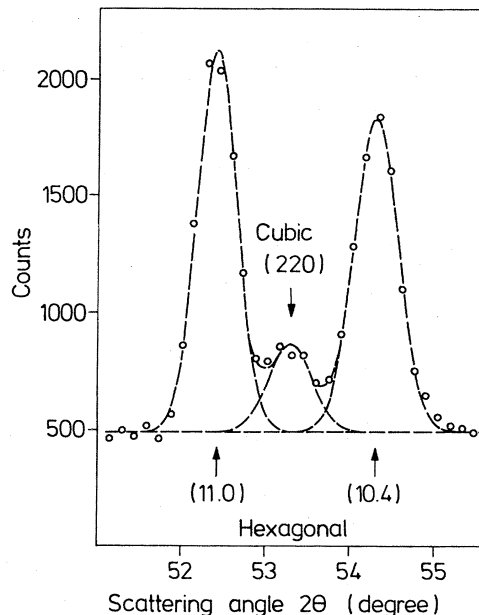


FIG. 1. Splitting of the (220) reflex in  $V_2Zr$  at low temperatures as observed by neutron scattering on sample S3; in this sample, the unsplit cubic remainder is about 12%. The data have been fitted by three Gaussians (dashed lines).

metry in the intensities of the split lines (see Fig. 1) is also present in the diffraction pattern of Ref. 9. Probably, atomic displacements within the rhombohedral unit cell lead to small changes in the structure factors.

We also tried to detect the martensitic transformation by x-ray powder diffraction as a function of temperature, using both Cu  $K\alpha$  and Mo  $K\alpha$  radiation, but without success. Even on powder samples (grain size 10–100  $\mu\text{m}$ ) we could not find any trace of line splitting at low temperatures. Obviously, in our sample the transformation is prevented in the neighborhood of a surface while bulk susceptibility measurements still indicated transforming material. This underlines the necessity of probing the *bulk*.

Finally, we note that to some extent, the bulk fraction  $p_{rh}$  of the transformed phase can be further increased by slower cooling or by repeated cooling cycles (“training”). We investigated this in an additional neutron scattering experiment on a virgin sample. We found this effect to be of the correct order of magnitude to explain the fact that

TABLE I. Bulk fractions  $p_{rh}$  of rhombohedral phase in S1 to S4 as determined by neutron scattering ( $n$ ), specific heat ( $c$ ), and magnetic susceptibility ( $\chi$ ) measurements.

Sample	$p_{rh}(n)$	$p_{rh}(c)$	$p_{rh}(\chi)$
S1		$0.58 \pm 0.06$	0.58
S2	$0.70 \pm 0.10$	$0.80 \pm 0.04$	0.73
S3	$0.88 \pm 0.02$	$0.96 \pm 0.005$	$0.96^a$
S4		$0.90 \pm 0.01$	

<sup>a</sup>Value assumed from specific-heat results; see text.

$p_{rh}^{\#}$  as extracted from neutron scattering data was slightly lower than  $p_{rh}$  as determined from specific-heat and susceptibility data. (Neutron scattering was always performed *first* and after rather rapid cooling.)

#### IV. SPECIFIC HEAT

Specific-heat data were taken on S1 to S4 in a heat-pulse calorimeter. On S4, additional measurements in a magnetic field of 13 T were performed in a superconducting magnet. Temperatures in zero field were determined by an unencapsulated glass-carbon thermometer calibrated in each run against a calibrated encapsulated glass-carbon thermometer from Lakeshore, and those in field by both the known<sup>10</sup> magnetoresistance of the glass-carbon element and a capacitance thermometer from Lakeshore. We checked our calibration by measuring the specific heat of a 212-mg high-purity sample of germanium both in 0 and 13 T and comparing with published values.<sup>11</sup> From this, we estimate the accuracy for our specific-heat data in 0 and 13 T to be within 3% with an error of about  $\pm 50$  mK in temperature.

In Fig. 2,  $C(T)/T$  versus  $T^2$  is shown in zero field for S1 to S4. Figure 3 shows the corresponding plot for S4 with and without magnetic field. For zero field, all curves display two distinct superconducting transitions. We identify the lower transition as that of the rhombohedral phase, and designate by  $\Delta C_{rh}$  and  $T_c^{rh}$ , respectively, the discontinuity in  $C(T)$  and the transition temperature of this phase. Accordingly, the higher transition (with  $\Delta C_{cub}$  and  $T_c^{cub}$ ) is identified as that of the cubic phase. These identifications are of central importance for

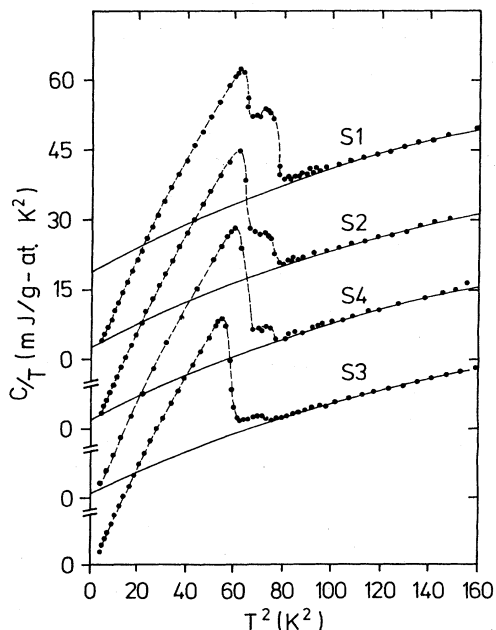


FIG. 2. Specific-heat data on S1 to S4 shown as  $C/T$  versus  $T^2$ ; in all four samples, two distinct superconducting transitions are clearly recognizable, the upper (lower) belonging to the cubic (rhombohedral) phase. Solid lines, fits of the normal state data; dashed lines, guides to the eye.

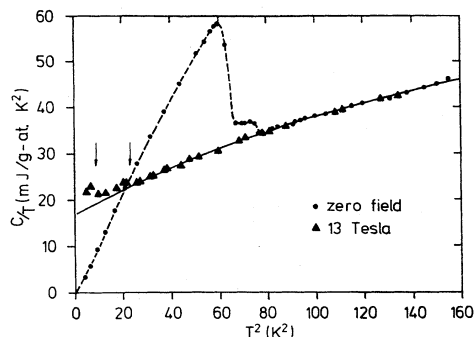


FIG. 3. Specific-heat results on S4 with and without magnetic field; the two arrows indicate the positions to which the two superconducting transitions have been depressed by the applied field; solid line, fit of the normal-state data; dashed line, guide to the eye. No suppression of the normal state  $C$  by the applied field is observed, consistent with the recent results for other spin fluctuators, e.g., Pd, in fields up to 20 T (Ref. 22).

the discussion below. They are based on the quantitative determination of the cubic and rhombohedral-phase percentages through our neutron-diffraction experiments and magnetic susceptibility measurements (see below). Regarding the data taken in magnetic field, the lower transition is clearly recognizable at  $\sim 3$  K, while the weak step at  $\sim 5$  K could be interpreted as an indication of the higher transition, in fair agreement with the results of Levinson.<sup>12</sup>

In the normal state, the experimental results were analyzed by fitting them to

$$C_N(T) = \gamma T + \beta T^3 + \alpha T^5, \quad (1)$$

with the usual requirement that the entropy above  $T_c^{cub}$  be independent of the superconducting phase transition. The resultant  $T_c$ ,  $\gamma$ , and  $\Theta_D = (12\pi^4 n k_B / 5\beta)^{1/3}$  are listed in Table II. In zero field, all our  $T_c$ 's are rather high, making the extrapolation of (1) down to  $T=0$  *a priori* doubtful. A check of this extrapolation is provided for S4 by depressing  $T_c$  below 5 K in a magnetic field. As demonstrated in Fig. 3, for this sample the extrapolation from above 8.8 K proves to be exact down to about 5 K, leaving little doubt that the  $\gamma$  values of the other samples are reliable, too. In order to extract the phase fraction  $p_{rh}$  and  $p_{cub}$  of rhombohedral and cubic phase, respectively, from our specific-heat data and to calculate the respective  $\gamma$  and  $\Delta C$ , we made use of the relations

TABLE II. Superconducting transition temperatures  $T_c$ , and specific-heat coefficients  $\gamma$  and  $\Theta_D$  for S1 to S4 in zero field and for S4 in a magnetic field of 13 T.

Sample	$T_c^{cub}$ (K)	$T_c^{rh}$ (K)	$\gamma$ (mJ/g-at. K <sup>2</sup> )	$\Theta_D$ (K)
S1	8.7	8.0	18.9	189
S2	8.7	8.0	17.8	195
S3	8.5	7.7	16.2	203
S4	8.7	8.0	17.0	195
S4 (13 T)	$\sim 5$	2.7	17.0	195

$$\gamma = p_{\text{rh}}\gamma_{\text{rh}} + p_{\text{cub}}\gamma_{\text{cub}}, \quad (2a)$$

$$\Delta C_{\alpha} = 1.43p_{\alpha}\gamma_{\alpha}T_c^{\alpha}\epsilon_{\alpha}, \quad (2b)$$

where  $\alpha$  stands for rh or cub and where  $\epsilon_{\alpha}$  allows for possible strong-coupling corrections to the BCS result. Since S3 transformed almost completely,  $\gamma_{\text{rh}}$  and  $\epsilon_{\text{rh}}$  could be determined virtually independently of the first guess made for  $\gamma_{\text{cub}}$  and  $p_{\text{cub}}$  and we found  $\gamma_{\text{rh}} = 16.1 \pm 0.5$  mJ/g-at. $\text{K}^2$  and  $\epsilon_{\text{rh}} = 1.3$ . Assuming<sup>13</sup>  $\epsilon_{\text{rh}}/\epsilon_{\text{cub}} = 1.0 \pm 0.2$ ,  $\gamma_{\text{cub}}$  was calculated from the data for S1 (the sample with the highest cubic remainder) to be  $23 \pm 1$  mJ/g-at. $\text{K}^2$ . A reduction of the quoted error bars by including the results for S2 and S4 is not possible. Since these samples have rather low cubic-phase fractions, they could only be used to provide information on the rhombohedral phase, which was already known from the results for S3 with much higher accuracy. The final values for  $p_{\text{rh}}$  from specific heat are listed in Table I.

Our results compare well with those by Rapp and Vieiland,<sup>6</sup> as far as  $\gamma_{\text{rh}}$  and  $T_c^{\text{rh}}$  are concerned. Indeed, these authors also reported two distinct discontinuities in their specific-heat data, but were unable to identify the minor phase (volume fraction  $\sim 7\%$ ,  $T_C \sim 8.5$  K) or to determine its  $\gamma$ . In our opinion, their minor phase is very likely to have been cubic  $\text{ZrV}_2$  as observed in all of our samples.

## V. MAGNETIC SUSCEPTIBILITY

The magnetic susceptibility  $\chi(T)$  was determined from magnetization measurements in fields up to 5 T using a Faraday balance which allowed us to eliminate traces of (ferromagnetic) impurities. The Faraday balance was calibrated against the known susceptibility of high-purity silver.<sup>12,14</sup> The absolute accuracy which is mainly determined by the error in the position of the sample in the magnetic field of the solenoid was estimated to be 2.5%. The relative accuracy of  $\chi(T)$  in an experiment with no change of the sample was better than 0.2%. Data were taken within the temperature range  $20 \leq T \leq 260$  K in steps of 10 K below 100 K, 5 K in the range  $100 < T < 130$  K, and 20 K above 140 K. The error in temperature measurements was less than 0.2%.

Measurements have been performed on samples S1 to S3. The corresponding  $\chi$  versus  $T$  curves are shown in Fig. 4. They all exhibit similar behavior:  $\chi(T)$  is strongly temperature dependent over the whole range with a precipitous decrease around  $T_M \sim 110$  K, the temperature where the martensitic phase transformation occurs. For S3, our data are very similar to those published by Marchenko and Polovov.<sup>7</sup> Following these authors, we assign the sharp drop around  $T_M$  to a lowering of the spin susceptibility  $\chi^s(T)$  in the rhombohedral phase and assume the orbital contribution  $\chi^o$  to be constant and equal to  $\chi^o \sim 1.8 \times 10^{-4}$  emu/g-at. for both phases. In order to determine the low-temperature susceptibility of the cubic phase, we make use of the theoretical calculation of  $\chi_{\text{cub}}^s(T)$  by Klein *et al.*<sup>4</sup> to extrapolate this quantity from  $T > 100$  K down to 20 K (see Fig. 4). This gives  $\chi_{\text{cub}}^s \sim 2.1 \times 10^{-4}$  emu/g-at. Since S3 is the sample with the highest amount of rhombohedral phase,  $\chi_{\text{rh}}^s(20)$  is best

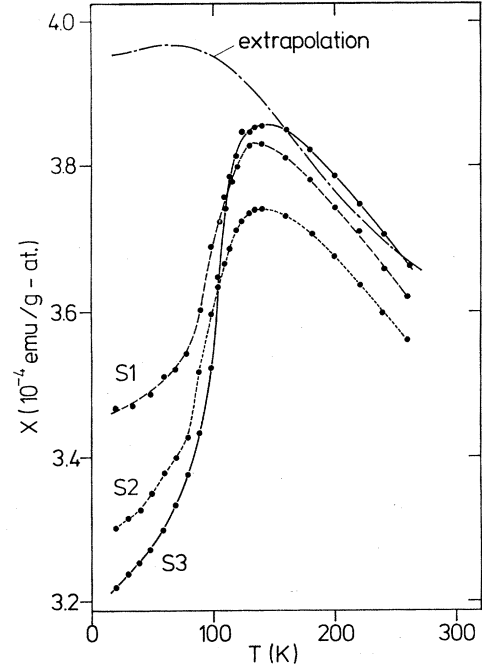


FIG. 4. Magnetic susceptibility  $\chi(T)$  versus temperature for S1 to S3; the chain line extrapolates  $\chi(T)$  for the cubic phase following Ref. 4. The small differences in  $\chi(T)$  for  $T > 130$  K (completely cubic phase) among the samples may be due to both slightly different positioning of the samples in the field gradient and small changes in stoichiometry, but note that our interest is mainly focused on the individual depression of  $\chi$  below  $T_M$  for each sample.

extracted from the data taken on S3. Making use of the decomposition

$$\chi^s(20) = p_{\text{rh}}\chi_{\text{rh}}^s(20) + (1 - p_{\text{rh}})\chi_{\text{cub}}^s(20), \quad (3)$$

and assuming  $p_{\text{rh}} \sim 0.96$  in S3 (from the specific-heat data, see Table I), we obtained  $\chi_{\text{rh}}^s(20) \sim 1.4 \times 10^{-4}$  emu/g-at. From these numbers,  $p_{\text{rh}}$  for S1 and S2 can readily be determined via Eq. (3) (see Table II). We did not give any error bars to these numbers which are all based on a rather rough guess for  $\chi^o$ . We emphasize, however, that the reason for our susceptibility measurements was not the determination of  $\chi_{\text{cub}}$  and  $\chi_{\text{rh}}$ , which were already known from Refs. 7 and 4. Rather, our interest was focused on the rhombohedral and cubic phase portions  $p_{\text{rh}}$  and  $p_{\text{cub}}$  for the different samples, since confirmation of these numbers is of vital importance for phase identifications and thus for our conclusions.

## VI. DISCUSSION AND CONCLUSIONS

Regarding the fractions of rhombohedral phase,  $p_{\text{rh}}$ , as deduced by different methods for our samples S1–S4 (see Table I), a clear correlation shows up: The amount of remaining cubic phase at low temperature is reflected quantitatively by the results of three different measurements independent of each other. Small discrepancies (regarding mainly the neutron scattering results) can be explained by training effects, different cooling cycles, and

texture. Thus a clear identification of the amounts of the two phases is possible. This allows us to assign unequivocally distinct values for  $\gamma$ ,  $\chi^s(20)$ , and  $T_c$  to both the cubic and the rhombohedral phase. We consider this to be our main success, particularly, when contrasted with earlier work on  $\text{Nb}_3\text{Sn}$ .<sup>15</sup> Those experiments aimed at determining  $\gamma$  and  $T_c$  of the cubic and tetragonal phase of this compound, but failed insofar as they did not allow the observation of two distinct discontinuities in the specific heat. Only the superconducting transition of the tetragonal phase in  $\text{Nb}_3\text{Sn}$  could be observed, leaving  $T_c$  for the cubic phase unclear. The reason for this may be found in the fact that in  $\text{Nb}_3\text{Sn}$  a considerable amount of impurities or defects is needed to stabilize the cubic phase at low temperatures. As a consequence, this phase in  $\text{Nb}_3\text{Sn}$  is no longer well defined, but rather consists of a distribution of phases with different  $T_c$ 's, thus smearing out the discontinuity in the specific heat. Contrary to this, from the present experiments we know that very small amounts of residual strain or stoichiometry variations are able to stabilize the cubic phase of  $\text{V}_2\text{Zr}$ , which remains well defined with a sharp superconducting transition.

Our central result is the observation that whereas both  $\gamma$  and  $\chi^s(20)$  are lowered by about 30% in the rhombohedral phase, the respective  $T_c$ 's of the cubic and rhombohedral phase differ by only 0.7 K. In view of the fact that at least for medium coupling strength  $\lambda$ ,  $T_c$  depends exponentially on  $\lambda$ , this is an almost negligible change. In the sense of what has been outlined in the Introduction, it indicates that  $dT_c/dN(0) \sim 0$  in  $\text{V}_2\text{Zr}$ , i.e., that this system is very close to an optimum situation for  $T_c$  with respect to changes in the electronic density of states at  $\epsilon_F$ . Let us analyze this further in terms of the quasiparticle DOS,  $N(\gamma)$  and  $N(\chi)$ , as defined by

$$\begin{aligned} N(\gamma) &= 3\gamma/2\pi^2 k_B^2, \\ N(\chi) &= \chi^s(20)/2\mu_B^2. \end{aligned} \quad (4)$$

From these quantities, the mass enhancement factor  $(1+\lambda) = N(\gamma)/N(0)$  and the Stoner enhancement factor  $S = N(\chi)/N(0)$  can be deduced if the bare DOS  $N(0)$  is

known. In both Refs. 4 and 5, a value for  $N(0)$  of about 110 states/spin Ry unit-cell has been given for the cubic phase of  $\text{V}_2\text{Zr}$ , while there exists no band-structure calculations for the rhombohedral phase. Following Ref. 4, one may obtain a guess for  $N(0)$  in the rhombohedral phase if one assumes the exchange interaction  $U$  which enters the Stoner factor  $S$  via

$$S = 1/[1 - N(0)U] \quad (5)$$

is the same for both phases. Then  $U$  can be fixed for the cubic phase, and for the rhombohedral phase we find  $N(0) \sim 91$  states/spin Ry unit-cell, i.e., a 20% reduction relative to its value in the more symmetric cubic phase.

What is striking is the very high mass enhancement in both phases. If  $\lambda$  were interpreted as being solely due to electron-phonon coupling,  $\lambda_{e\text{-ph}} \sim 2.6$  would result for the cubic phase. Together with  $\Theta_D \sim 200$  K, such a large value would lead to a much higher  $T_c$  than the actual 8.7 K if the Coulomb interaction were treated by the usual  $\mu^*$  approach with  $\mu^* \sim 0.1$ . Indeed, starting from a McMillan-type  $T_c$  formula, both Refs. 4 and 5 arrived at a  $T_c$  for cubic  $\text{V}_2\text{Zr}$  that was a factor of 2–4 higher than the observed 8.7 K. On the other hand, for the cubic phase our  $N(\chi)/N(0)$  gives  $S \sim 2.4$  (Klein *et al.*<sup>2</sup> even calculated  $S \sim 3.8$ ) which indicates a strong pair-breaking influence of spin fluctuations. This means that in  $\text{V}_2\text{Zr}$ ,  $dT_c/dN(0) \sim 0$  because of an almost complete balance between strong ( $\lambda > 1$ ) electron-phonon coupling and spin fluctuations. This idea is further corroborated by the fact that the ratio  $N(\chi)/N(\gamma) = S/(1+\lambda)$  is about the same ( $\sim 0.7$ ) for both phases in contrast to the strong individual variations of  $N(\gamma)$  and  $N(\chi)$ , but in accordance with the almost unchanged  $T_c$ .

The appearance of spin fluctuations in  $\text{V}_2\text{Zr}$  does not come as a surprise. As a vanadium-based superconductor with a high electronic DOS,  $\text{V}_2\text{Zr}$  is akin to V, VN,  $\text{V}_3\text{Ga}$ , and  $\text{V}_3\text{Si}$ , where indications for the coexistence of spin fluctuations and superconductivity have already been reported.<sup>16–21</sup> What makes  $\text{V}_2\text{Zr}$  a particularly intriguing further example is the possibility of studying the competition between electron-phonon coupling and spin fluctuations during a change (cubic  $\rightarrow$  rhombohedral) in the system.

<sup>1</sup>R. C. Dynes and C. M. Varma, *J. Phys. F* **6**, L215 (1976).

<sup>2</sup>B. Stritzker, *Phys. Rev. Lett.* **42**, 1769 (1979).

<sup>3</sup>K. Kai, T. Nakamichi, and N. Yamamoto, *J. Phys. Soc. Jpn.* **25**, 1192 (1968).

<sup>4</sup>B. M. Klein, W. E. Pickett, D. A. Papaconstantopoulos, and L. L. Boyer, *Phys. Rev. B* **27**, 6721 (1983).

<sup>5</sup>T. Jarlborg and A. J. Freeman, *Phys. Rev. B* **22**, 2332 (1980).

<sup>6</sup>O. Rapp and L. J. Vieland, *Phys. Lett. A* **36**, 369 (1971).

<sup>7</sup>V. A. Marchenkov and V. M. Polovov, *Zh. Eksp. Teor. Fiz.* **78**, 1062 (1980) [*Sov. Phys.—JETP* **51**, 535 (1980)].

<sup>8</sup>F. J. Rotella, H. E. Flotow, D. M. Gruen, and J. D. Jorgensen, *J. Chem. Phys.* **79**, 4522 (1983).

<sup>9</sup>D. E. Moncton, *Solid State Commun.* **13**, 1779 (1973).

<sup>10</sup>H. H. Sample, B. L. Brandt, and L. G. Rubin, *Rev. Sci. Instrum.* **53**, 1129 (1982).

<sup>11</sup>P. Flubacher, A. J. Leadbetter, and J. A. Morrison, *Philos. Mag.* **4**, 273 (1959).

<sup>12</sup>M. Levinson, Thesis, Massachusetts Institute of Technology, 1978.

<sup>13</sup>H. Rietschel, *Phys. Rev. B* **24**, 155 (1981). In this paper, it has been shown that the deviation function  $D(T/T_c)$  in V and VN is insensitive to any simultaneous rescaling of  $\lambda$  and  $S$  which leaves  $T_c$  unaltered. Since  $\epsilon$  is directly related to  $D(T/T_c)$ , and since in several regards  $\text{V}_2\text{Zr}$  is similar to VN, we believe the assumption  $\epsilon_{\text{th}}/\epsilon_{\text{cub}} \sim 1.0 \pm 0.2$  to be reasonable.

<sup>14</sup>M. Garber, W. G. Henry, and H. G. Hoeve, *Can. J. Phys.* **38**,

- 1595 (1960).
- <sup>15</sup>A. Junod, J. Muller, H. Rietschel, and E. Schneider, *J. Phys. Chem. Solids* **39**, 317 (1978).
- <sup>16</sup>T. P. Orlando, E. J. McNiff, S. Foner, and M. R. Beasley, *Phys. Rev. B* **19**, 4545 (1978).
- <sup>17</sup>H. Rietschel and H. Winter, *Phys. Rev. Lett.* **43**, 1256 (1979).
- <sup>18</sup>H. Rietschel, H. Winter, and W. Reichardt, *Phys. Rev. B* **22**, 4284 (1980).
- <sup>19</sup>T. P. Orlando and M. R. Beasley, *Phys. Rev. Lett.* **46**, 1598 (1981).
- <sup>20</sup>A. Junod, T. Jarlborg, and J. Muller, *Phys. Rev. B* **27**, 1568 (1983).
- <sup>21</sup>T. Jarlborg, A. Junod, and M. Peter, *Phys. Rev. B* **27**, 1558 (1983).
- <sup>22</sup>G. R. Stewart and B. L. Brandt, *Phys. Rev. B* **28**, 2266 (1983).